ARTICLE

Atmospheric pressure non-thermal plasma activation of CO_2 in a packed-bed dielectric barrier discharge reactor

D.H. Mei, and X. Tu*[a]

Abstract: Direct conversion of CO_2 into CO and O_2 was carried out in a packed-bed dielectric barrier discharge (DBD) non-thermal plasma reactor at low temperatures and atmospheric pressure. The maximum CO_2 conversion of 22.6% was achieved when $BaTiO_3$ pellets were fully packed into the discharge gap. The introduction of γ-Al_2O_3 or 10 wt.% Ni/γ-Al_2O_3 catalyst into the $BaTiO_3$ packed DBD reactor increased both CO_2 conversion and energy efficiency of the plasma process. Packing γ-Al_2O_3 or 10 wt.% Ni/γ-Al_2O_3 in the upstream of the $BaTiO_3$ bed showed higher CO_2 conversion and energy efficiency compared to that using middle or downstream packing modes as the reverse reaction of CO_2 conversion – the recombination of CO and O to form CO_2 is more likely to happen in the middle and downstream modes. Compared to the γ-Al_2O_3 support, the coupling of the DBD with the Ni catalyst showed a higher CO_2 conversion which can be attributed to the presence of Ni active species on the catalyst surface. The argon plasma treatment of the reacted Ni catalyst provided extra evidence to confirm the role of Ni active species in the conversion of CO_2.

1. Introduction

The increasing energy demand in the modern society has caused a large consumption of conventional carbon-containing fossil fuels, which consequently releases significant amounts of greenhouse gases (mainly CO_2) into atmosphere. In 2013, the concentration of CO_2 in the atmosphere (~ 400 ppm) was 42% more than that of preindustrial level [1]. CO_2 has been considered as the main contributor to global warming and greenhouse effect, resulted in catastrophic effects to the ecosystem. The UK government has committed to reduce greenhouse gas emissions by at least 80% (from the 1990 baseline) by 2050 [2]. Different innovative and cost-effective technologies are being developed to tackle the global challenge of CO_2 emissions, such as reducing fossil fuel consumption, increasing the use of alternative and renewable energy, carbon capture and storage (CCS) and carbon capture and utilization (CCU). CCU is a promising approach to sustainably reduce carbon emissions, as in this process, the captured and separated CO_2 serves as a feedstock to produce a wide range of value-added synthetic fuels and platform chemicals (e.g. liquid fuels) [3]. Direct decomposition of CO_2 (Equation 1) is a typical CO_2 conversion route and has gained increasing attention as CO is a critical chemical feedstock for the synthesis of liquid hydrocarbons, synthetic petroleum and oxygenates [4]. However, CO_2 is a highly stable and non-combustible molecule, considerable energy is thus required for upgrading and activation of CO_2, which will induce high energy cost in the conventional thermal or catalytic process for CO_2 conversion.

$$CO_2 \rightarrow CO + \frac{1}{2}O_2 \qquad \Delta H = 280\,\text{kJ/mol} \qquad (1)$$

Non-thermal plasma (NTP) technology provides a promising alternative solution for the conversion CO_2 into value-added fuels and chemicals at ambient conditions due to its distinct non-equilibrium character [5]. In non-thermal plasmas, the bulk gas temperature can be close to room temperature, while the generated electrons are highly energetic which collide with surrounding gas and produce a range of reactive species such as radicals, ions, excited atoms and molecules [6]. These energetic and reactive species can easily break most chemical bonds (e.g. C-O bonds) and enable thermodynamically unfavourable chemical reactions (e.g. CO_2 decomposition) to take place at ambient conditions in non-thermal plasmas. Various NTP systems have been used for the direct conversion of CO_2, such as dielectric barrier discharge (DBD) [5a, 7], corona discharge [8], glow discharge [9], gliding arc discharge [10] and microwave discharge [11]. Recently, the use of packed bed DBD reactors for CO_2 conversion has attracted significant interest as the presence of catalytic or non-catalytic packing materials in the discharge can effective intensify the local electric field near the contact points between the packing pellets and the average electric field in the plasma system, consequently enhances the process performance even using non-catalytic packing materials. The performance of a packed bed DBD reactor for chemical reaction is strongly dependent on the shape, size and physical and chemical properties (e.g. surface structure, adsorption capability and dielectric constant) of the packing materials [7m, 7n, 7p-r, 7t, 12]. Packing catalysts in a DBD reactor has great potential to enhance the performance of the plasma process due to the generation of both physical and catalytic effects of the catalysts on the reaction. Previous efforts were mainly devoted to investigating the effect of processing parameters (e.g. frequency, discharge power, dielectric materials, and feed flow rate, etc.) on the performance of plasma CO_2 processing in a packed bed DBD reactor [5a, 7c, 7d, 7h-j], while the knowledge of selecting a suitable catalyst which can be integrated into a DBD or packed bed DBD reactor for plasma CO_2 decomposition is largely unknown. Liu et al investigated CO_2 reduction to CO on different transition metal surfaces using a density function theory (DFT) method. They found that Ni surfaces are effective for CO_2 adsorption and decomposition in the reduction of CO_2 to CO [13]. Ni based catalysts have been used in plasma-catalytic CO_2 reforming of CH_4 and CO_2 hydrogenation [6a, 14]; while limited efforts have been placed on the investigation of Ni catalysts in plasma CO_2 decomposition [12]. Catalysts can be placed in a DBD reactor in different ways. However, it is still not clear how the location of a catalyst bed in a DBD reactor affects

[a] Dr. D.H. Mei, Dr. X. Tu
Department of Electrical Engineering and Electronics
University of Liverpool
Liverpool L69 3GJ
UK
Tel: +44-1517944513
E-mail: xin.tu@liverpool.ac.uk

the performance of plasma chemical reactions, especially the CO_2 conversion process.

In this work, direct conversion of undiluted CO_2 into CO and O_2 was carried out in a packed-bed dielectric barrier discharge (DBD) at low temperatures. The effect of CO_2 flow rate and discharge power on the CO_2 conversion was evaluated in the DBD reactor packed with $BaTiO_3$ pellets only. An extra packing bed (γ-Al_2O_3 or 10 wt.% Ni/γ-Al_2O_3) was placed in the different locations of the $BaTiO_3$ packed bed DBD reactor to understand the effect of different packing modes on the plasma conversion of CO_2. The effect of plasma treatment on the performance of the Ni/γ-Al_2O_3 catalyst in the CO_2 conversion process was also discussed.

2. Results and Discussion

2.1. Thermodynamic equilibrium analysis of CO_2 conversion process

The thermodynamic equilibrium calculation of CO_2 decomposition was carried out using the method based on minimization of Gibbs free energy in a closed system [15]. The details of this methodology can be found in previous literature [15a]. In the calculation, it was supposed that 1 mol of CO_2 was injected into the closed system. The final products include O_2 and CO which were identified as the only products in the experiment, while no ozone or carbon deposition was found. Figure 1 (a) shows the influence of reaction temperature and operating pressure on CO_2 conversion. Clearly, CO_2 begins to decompose near 2000 K with a low conversion of CO_2. Extraordinarily high temperatures (2500-3000 K) are required to reach a CO_2 conversion of 20-40%, which leads to a high energy cost for the conversion of CO_2 using thermal processes. Increasing operating pressure significantly decreases the conversion of CO_2 at a constant reaction temperature. The thermal energy efficiency of CO_2 conversion was calculated using the method described in previous literature [16], as shown in Figure 1 (b). A maximum energy efficiency for CO_2 conversion can be achieved at an operating temperature between 2900 K and 3700 K. Increasing operating pressure would shift the maximum energy efficiency to a lower value at a higher temperature. As shown in Figure 1, decreasing operating pressure is beneficial for achieving both high CO_2 conversion and energy efficiency. However, vacuum systems are required if the conversion process is operated at low pressures (e.g. 0.1 atm), which will increase the operation cost.

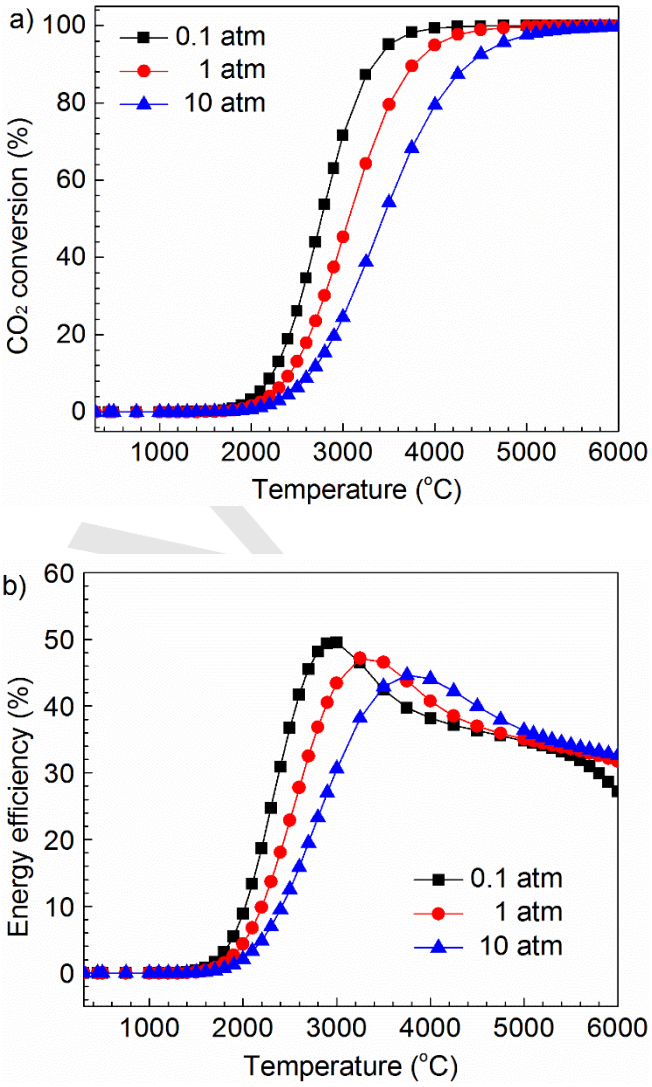

Figure 1. Thermodynamic equilibrium analysis of CO_2 conversion as a function of reaction temperature and operating pressure: a) CO_2 conversion; b) energy efficiency.

2.2. CO_2 conversion in a $BaTiO_3$ packed-bed DBD reactor

Figure 2 shows the influence of discharge power and CO_2 flow rate on the conversion of CO_2 and energy efficiency in the $BaTiO_3$ packed-bed DBD reactor (reference mode). Clearly, increasing discharge power or decreasing CO_2 flow rate increased the conversion of CO_2. The highest CO_2 conversion of 22.6% was obtained at the maximum discharge power of 40 W and a minimum CO_2 flow rate of 30 mL/min. Increasing the discharge power by changing the applied voltage at a fixed frequency in a DBD reactor can effectively increase the number of microdischarges generated in the DBD plasma, producing more chemical reaction channels and energetic species for CO_2 decomposition, and consequently enhanced the conversion of CO_2. In addition, decreasing CO_2 flow while keeping other parameters constant increased the residence time of CO_2 in the

discharge area and the possibility for CO_2 conversion through more collisions of CO_2 with energetic electrons and reactive species, resulted in the enhanced CO_2 conversion. Similar phenomenon was also reported in the plasma processing of CO_2 processing using a non-packed DBD reactor [17].

The effect of CO_2 gas flow and discharge power on the energy efficiency of the plasma process showed the opposite behavior. Increasing the CO_2 flow rate enhanced the energy efficiency of the plasma process although the conversion of CO_2 was lower at a higher CO_2 flow rate. In addition, the energy efficiency decreased by around 30% when increasing the discharge power from 20 to 40 W.

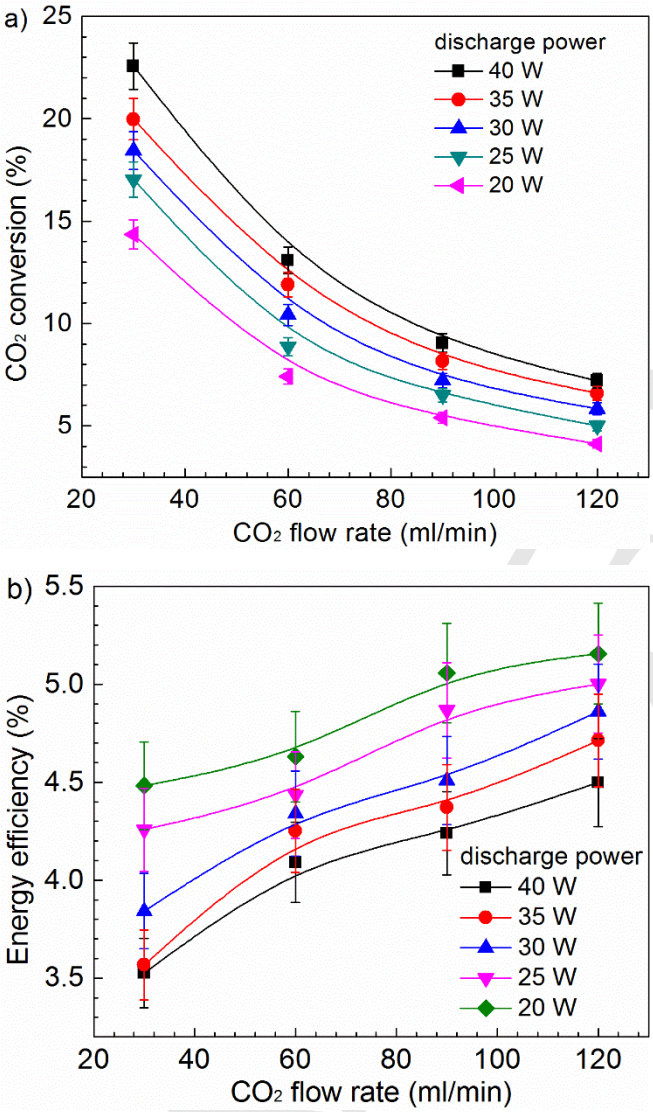

Figure 2. Effect of CO_2 flow rate and discharge power on a) CO_2 conversion and b) energy efficiency of the plasma process in the reference mode.

When the same experiment was carried out in the absence of the $BaTiO_3$ under similar operating conditions, a stable discharge could not be ignited in a pure CO_2 flow due to the presence of large discharge gap. This demonstrates that the presence of the packing material is vital for the process to take place under these experimental conditions. Previous results showed that the breakdown voltage of a CO_2 DBD was significantly decreased due to the reduced discharge gap when packing materials were fully packed in the discharge area [7p]. In addition, compared to the plasma conversion of CO_2 with no packing, the presence of the $BaTiO_3$ in the discharge can effectively enhance the CO_2 conversion [7p].

In the presence of packing materials, the discharge near the contact point between the packing pellets and between the pellets and the quartz wall was intensified, resulted in the enhanced electric field for chemical reactions. Our previous study found that the average electric field in a CO_2 DBD reactor fully packed with the $BaTiO_3$ (1 mm) was almost two times of that in the CO_2 discharge with no packing [7p], which increased the mean electron energy and therefore significantly enhanced the conversion of CO_2. Van Laer et al calculated the electric field distribution, electron temperature, and electron density in a DBD reactor packed with ZrO_2 beads by using a 2D fluid modeling [7q]. Their results showed that the local electric field near the contact points was stronger than that in the void (gas region). These findings can be ascribed to the accumulation of local charges of opposite sign at the contact point due to the polarization of the packing dielectric pellets by the applied potential difference between two electrodes. As a result, more highly energetic electrons could be generated for the conversion of CO_2 via electron impact dissociation [7q].

2.3. Effect of catalyst and different packing modes

Figure 3 shows the effect of γ-Al_2O_3 support and Ni/γ-Al_2O_3 catalyst on the conversion of CO_2 using different packing modes. Compared to the reaction using the $BaTiO_3$ only (reference mode), adding γ-Al_2O_3 support or Ni/γ-Al_2O_3 catalyst to the $BaTiO_3$ packed DBD reactor enhanced both the conversion of CO_2 and energy efficiency at the same discharge power. γ-Al_2O_3 is a typical amphoteric oxide, on which an acidic gas (e.g. CO_2) is preferably absorbed [7m]. The acid-basic property of γ-Al_2O_3 facilitates the adsorption, activation and conversion of CO_2. The positive effect of γ-Al_2O_3 packing on CO_2 conversion was reported using a pulsed corona discharge reactor [18] and similar packed-bed DBD reactors [7m, 7r]. The presence of the Ni/γ-Al_2O_3 catalyst in the discharge showed higher CO_2 conversion and energy efficiency compared to the same reaction over the γ-Al_2O_3 support, which can be attributed to the existence of active Ni species over the catalyst surface which contributed to the dissociation of CO_2 molecules over the Ni catalyst [13a]. Interestingly, the position of the catalyst bed affected the reaction performance in terms of the CO_2 conversion and energy efficiency of the plasma process. The highest CO_2 conversions (24.7% for γ-Al_2O_3 and 26.3% for Ni/γ-Al_2O_3) were obtained in the upstream mode.

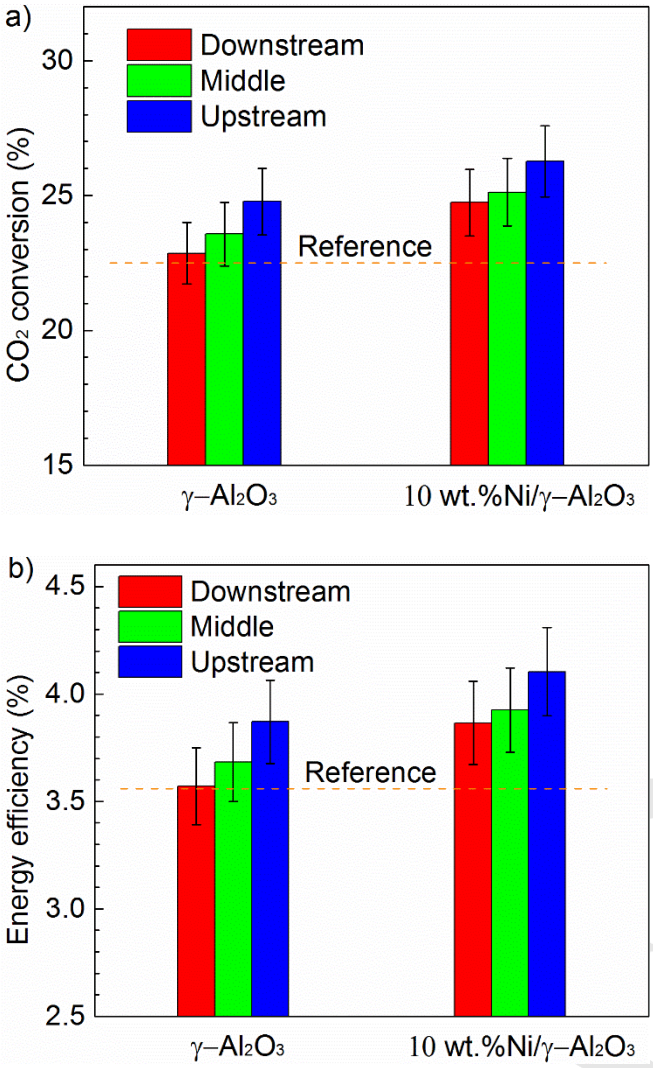

Figure 3. Effect of catalyst and support on a) CO_2 conversion and b) energy efficiency using different packing modes (discharge power: 40 W; CO_2 flow rate: 30 mL/min).

In this work, CO_2 decomposition was also carried out in the same DBD reactor with a 15 cm length of $BaTiO_3$ bed. The CO_2 conversion and energy efficiency was 30.9% and 4.8%, respectively, which were higher than the values obtained using a $BaTiO_3$ bed (12 cm) combined with an extra packing (3 cm, γ-Al_2O_3 or Ni/ γ-Al_2O_3 catalyst) placed in the different locations of the DBD reactor at the same discharge power and flow rate. These results suggest that $BaTiO_3$ is more effective for CO_2 decomposition compared to the γ-Al_2O_3 support and the Ni/ γ-Al_2O_3 catalyst in the plasma process. Our previous works showed the presence of $BaTiO_3$ in a DBD reactor significantly enhanced the conversion of CO_2 by around 250% which can be attributed to the physical effect (e.g. enhanced electric field) induced by the presence of $BaTiO_3$ with a high dielectric constant and the dominant photocatalytic surface reactions driven by the plasma [19]. Thus, the present work will mainly focus on the investigation of the effect of the Ni catalyst and packing location on the plasma conversion of CO_2.

This is mainly due to the higher dielectric constant of $BaTiO_3$ (~ 10000), compared to that of γ-Al_2O_3 (~ 9). Packing materials with high dielectric constants can significantly reduce the critical breakdown voltage in the DBD reactor. In our previous study, we found that $BaTiO_3$ beads into the plasma system enhanced the average electric field and mean electron energy of the CO_2 discharge by a factor of 2, which significantly contributed to the enhancement of CO_2 conversion and energy efficiency of the plasma process [7p]. Although the photocatalytic reactions on the $BaTiO_3$ surface for CO_2 conversion is non-negligible [7p, 19], the activation mechanism for CO_2 conversion in the extra $BaTiO_3$ bed and extra γ-Al_2O_3 (or Ni/γ-Al_2O_3) bed might be totally different, which could accounted for the difference of CO_2 conversion and energy efficiency in these conditions.

2.4. Argon plasma treatment of Ni catalyst

After running the experiment for 2 hours, the reacted Ni/γ-Al_2O_3 catalyst was treated by a pure Ar discharge for 30 min in the same DBD reactor at a discharge power of 40 W and an Ar flow rate of 50 mL/min. The plasma treated Ni/γ-Al_2O_3 catalyst was then used for CO_2 conversion in the same packed DBD reactor under the same experimental conditions as that used for testing the Ni/γ-Al_2O_3 catalyst. Figure 4 shows the conversion of CO_2 and energy efficiency using plasma treated and untreated Ni/γ-Al_2O_3 catalyst. Clearly, compared to the CO_2 conversion using the Ni catalyst, the use of the plasma treated spent Ni catalyst enhanced the CO_2 conversion and energy efficiency in both middle and upstream packing modes. For instance, in the upstream packing mode, the CO_2 conversion was increased by 8.5% when using the plasma treated Ni catalyst, compared to that using the catalyst reacted for 2 hours.

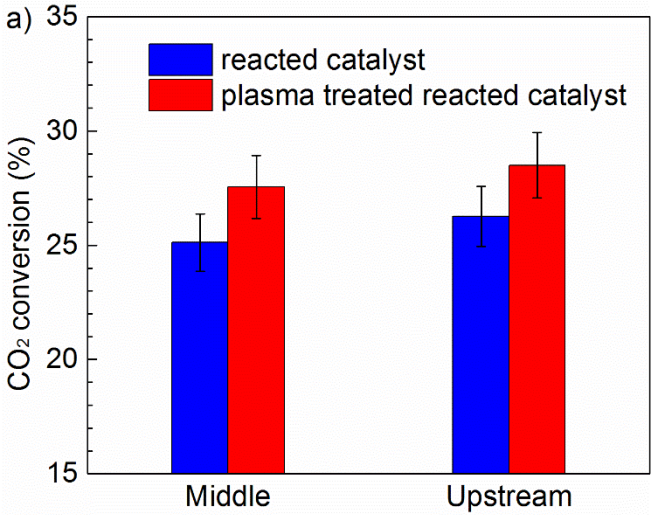

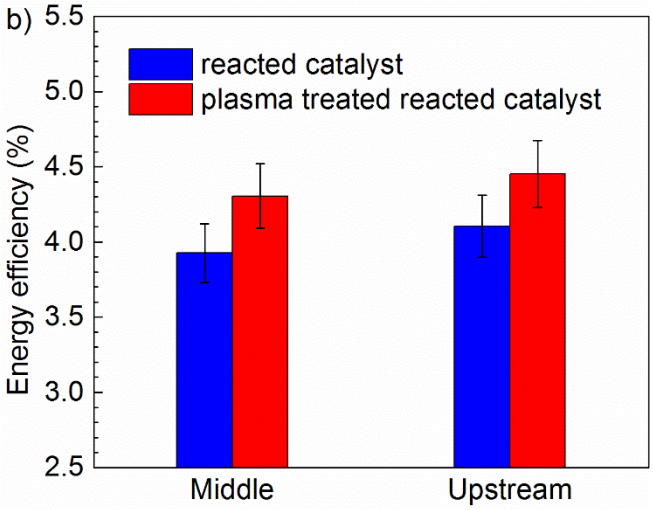

Figure 4. Effect of plasma treatment of the reacted Ni/γ-Al_2O_3 catalyst on a) CO_2 conversion and b) energy efficiency using different packing modes (discharge power: 40 W; CO_2 flow rate: 30 mL/min).

2.5. Discussion

Compared to the CO_2 conversion using the $BaTiO_3$ only (reference mode), adding γ-Al_2O_3 support or Ni/γ-Al_2O_3 catalyst to the $BaTiO_3$ packed-bed DBD reactor enhanced the conversion of CO_2 under the same operating conditions. Adding an extra packing bed (γ-Al_2O_3 or Ni/γ-Al_2O_3) in the discharge elongated the residence time of CO_2 in the reaction zone although the power density of the reactor was decreased due to the increase of the discharge volume at the same discharge power. Clearly, the change of the residence time had a more prominent effect on the conversion of CO_2. One may argue that the increase of the bed length when using the extra γ-Al_2O_3 or Ni/γ-Al_2O_3 bed was the main factor that led to the enhanced CO_2 conversion and energy efficiency compared to those in the reference mode. The coupling of the DBD with the Ni/γ-Al_2O_3 catalyst showed higher CO_2 conversion and energy efficiency compared to the same reaction over the γ-Al_2O_3 support regardless of the packing modes used, which indicates that the catalytic effect of Ni surfaces cannot be ruled out: dissociation of CO_2 molecules over the Ni active sites on the surface of the catalyst [13a]. In the plasma CO_2 conversion coupled with the Ni catalyst, both gas phase reactions and plasma-assisted surface reactions were contributed to the conversion of CO_2. In addition to the electron impact dissociation of CO_2 (Equation 2) in the plasma gas phase, CO_2 molecules in both ground and excited states can be absorbed onto the Ni surfaces to form CO_{2ad}, which will be dissociated into CO_{ad} and O_{ad} with the aid of energetic electrons (Equation 3). The CO_{ad} will be desorbed, releasing CO; while the O_{ad} will be recombined to O_{2ad} (Equation 4), followed by desorption to release O_2. The CO_{ad} and O_{ad} species can also be formed by adsorption of CO and O radicals from the gas phase onto the catalyst surface. The reverse reaction – the recombination of CO (or CO_{ad}) and O (or O_{ad}) to form CO_2 (Equations 5 - 8) cannot be ruled out. However, it is reported that the recombination of O radicals to form O_2 prevails over the recombination of CO with O radicals on the solid surfaces at low temperatures [12].

$$e + CO_2 \rightarrow CO + O + e \quad (2)$$
$$e + CO_{2ad} \rightarrow CO_{ad} + O_{ad} + e \quad (3)$$
$$O_{ad} + O_{ad} \rightarrow O_{2ad} \quad (4)$$
$$CO_{ad} + O_{ad} \rightarrow CO_2 \quad (5)$$
$$CO_{ad} + O \rightarrow CO_2 \quad (6)$$
$$CO + O_{ad} \rightarrow CO_2 \quad (7)$$
$$CO + O + M \rightarrow CO_2 + M \quad (8)$$

The results showed that the location of the packing bed (γ-Al_2O_3 or Ni/γ-Al_2O_3) played an important role in determining the reaction performance. Packing γ-Al_2O_3 or Ni/ γ-Al_2O_3 in the upstream of the $BaTiO_3$ bed showed higher CO_2 conversion compared to the same reaction using either middle or downstream packing mode. Note that the initial present reactant before entering the catalyst packing bed was different for different packing modes. For example, CO_2 was the only initial reactant before the catalyst packing bed in the upstream mode, while in the middle and downstream modes, the initial reactants include CO, O_2 and CO_2. The presence of the extra packing bed in the middle and downstream modes provided more chance for the recombination of CO and O to form CO_2 through Equation 5 to 8, a competing reaction for CO_2 decomposition in the plasma process. This could be the reason to get reduced CO_2 conversion when placing the extra bed in the middle or downstream of the $BaTiO_3$ bed. In addition, Ni particles on the catalyst surface could be re-oxidized due to the formation of oxygen in the process, reducing the catalyst activity and thus the conversion of CO_2, especially for the middle and downstream modes.

The effect of the Ni active species on the CO_2 conversion can also be evidenced from the argon plasma treatment of the reacted Ni catalyst. The plasma treated Ni catalysts showed higher CO_2 conversion and energy efficiency compared to the reacted Ni catalyst used for 2 hours, which could be re-oxidized to form NiO due to the presence of oxygen. During the plasma reaction using the fresh Ni/γ-Al_2O_3, the Ni particle size might be decreased [12, 20]. The decrease in Ni particle size was beneficial to the re-utilization of the catalysts. In non-thermal plasmas, the gas kinetic temperature remains low (as low as room temperature), thus the thermal effect can be neglected in the plasma treatment process. In the argon plasma treatment of the Ni catalyst, highly energetic electrons and metastable argon species (Ar*) are considered as the key driving force to reduce metal oxide to metal on the catalyst surface [21]. The re-oxidized Ni/γ-Al_2O_3 catalyst could be reactivated through the argon plasma reduction process. In addition, the highly energetic electrons and metastable argon species (Ar*) in the plasma could affect the interactions between the Ni particles and γ-Al_2O_3, and consequently enhance the distribution of Ni particles on the catalyst surface.

The energy efficiency of CO_2 conversion using DBDs is relatively lower than that using microwave discharges or gliding arc plasmas. A maximum energy efficiency of 17.5% for CO_2 conversion (42% conversion) was reported using a low pressure (10 Torr) microwave discharge combined with a NiO/TiO_2 catalyst [11b]. However, it is difficult to achieve such a high energy efficiency for CO_2 conversion at atmospheric pressure, whilst low pressure

systems are more complicated and costly. In atmospheric pressure gliding arc plasma systems, the high energy efficiency is generally obtained at the expense of a relatively low CO_2 conversion. Indarto et al. reported a maximum energy efficiency of ~19% for CO_2 conversion using a gliding arc discharge at a CO_2 flow rate of 0.86 l/min, which corresponds to a relative low CO_2 conversion (~15%) [10a].

DBD has the advantage of its flexibility and simplicity for coupling with appropriate catalysts, especially for the synthesis of value-added platform chemicals and synthetic fuels (e.g. oxygenates) from CO_2 at ambient conditions. The combination of the plasma with the catalysts has great potential to generate plasma-catalytic synergy, which can further enhance the conversion and energy efficiency of the plasma process, especially breaking the trade-off barrier between the conversion and energy efficiency present in plasma chemical processes. The capability of scaling up for DBD reactors has been demonstrated in large scale plasma processes for water treatment, gas cleaning and ozone generation [22]. Therefore, DBD has the potential to be scaled-up for CO_2 conversion and utilization. Significant efforts are required for the further investigation and optimization of the plasma CO_2 conversion process through both experimental and modeling approaches [7h, 17, 23]. In addition, the integration of the plasma process with renewable energy sources (e.g. solar and wind energy) would provide a promising route of chemical energy storage for surplus electricity during the peak moment on the grid [24] and a sustainable alternative to reduce CO_2 emission.

3. Conclusions

In this work, plasma decomposition of CO_2 into CO and O_2 was carried out in the $BaTiO_3$ packed-bed DBD reactor. Compared to the reaction using the $BaTiO_3$ only (reference mode), adding γ-Al_2O_3 or 10 wt.% Ni/γ-Al_2O_3 catalyst to the $BaTiO_3$ packed DBD reactor enhanced both CO_2 conversion and energy efficiency of the plasma process. The coupling of the discharge with the 10wt.% Ni/γ-Al_2O_3 catalyst showed higher CO_2 conversion and energy efficiency in comparison to that using γ-Al_2O_3 support. The results showed that the location of the catalyst bed played a key role in determining the process performance. Compared to the middle and downstream packing modes, placing an extra packing bed (γ-Al_2O_3 or Ni/γ-Al_2O_3) in the upstream of the $BaTiO_3$ bed showed higher CO_2 conversion and energy efficiency. Due to the presence of different reactant compositions before entering the extra packing bed using different packing modes, the recombination of CO and O to form CO_2, a reverse reaction for CO_2 conversion, is more likely to happen on the catalyst or support surface in the middle and downstream modes, which leads to lower CO_2 conversion against that obtained in the upstream packing mode. The results of the argon plasma treatment of the reacted Ni catalyst provided further evidence to support the role of the Ni active sites in the dissociation of CO_2, which showed the Ni/γ-Al_2O_3 catalyst had a higher CO2 conversion than that using γ-Al_2O_3.

Experimental Section

Experimental setup

The experiments were carried out in a packed-bed DBD reactor, as shown in Figure 5 (a). An Al foil (ground electrode) was wrapped over a quartz tube with an external diameter of 25 mm and an inner diameter of 22 mm. A stainless-steel rod with an outer diameter of 6 mm was used as an inner electrode (high voltage electrode). As a result, the discharge gap was 8 mm in the absence of packing materials.

The DBD reactor was connected to an AC high voltage power supply with a peak-to-peak voltage of 10 kV and a fixed frequency of 50 Hz. All the electrical signals (applied voltage, current and voltage on the external capacitor) were recorded by a four-channel digital oscilloscope (TDS2014). The discharge power was calculated by using the Q-U Lissajous figure. A homemade online power measurement system was used to control the discharge power in real time. The discharge power can be adjusted by changing the applied voltage at a fixed frequency.

Three different packing materials $BaTiO_3$ (TCU), γ-Al_2O_3 (Alfa Aesar) and 10 wt.% Ni/γ-Al_2O_3 with a diameter of 3 mm were evaluated in the plasma conversion of CO_2. The 10 wt.% Ni/γ-Al_2O_3 catalyst was prepared using the wetness impregnation method [14b]. $Ni(NO_3)_2{\cdot}6H_2O$ (Alfa Aesar) was used as the metal precursor. Initially, the nickel nitrate was dissolved in the deionized water and stirred at room temperature for 1 h to obtain a 0.1 M solution. The appropriate weight of γ-Al_2O_3 (3 mm diameter beads) was added to the metal precursor solution and impregnated for 12 h. After that, the solution containing γ-Al_2O_3 beads was evaporated at 80 °C for 4 h and dried at 110 °C overnight, followed by the calcination at 400 °C for 4 h. Prior to the plasma reaction, the Ni catalyst was reduced in an Ar-H_2 plasma for 30 mins at a discharge power of 40 W and a total flow rate of 50 mL/min with 20 vol.% H_2 in the same DBD reactor. Previous work demonstrated that NiO can be reduced to Ni on the catalyst surface using a similar Ar/H_2 DBD [25]. In addition, the γ-Al_2O_3 pellets were dried at 110 °C overnight to remove moistures before the plasma reaction.

Different packing modes were used to understand the effect of the location of catalyst bed on the plasma conversion of CO_2, as shown in Figure 1 (b). In the reference mode, only $BaTiO_3$ pellets were fully packed into the discharge area with a discharge length of 120 mm, while γ-Al_2O_3 (or Ni/γ-Al_2O_3) packing bed can be placed in the upstream, middle and downstream of the $BaTiO_3$ bed, forming three different packing modes: upstream mode, middle mode and downstream mode, respectively. The length of the γ-Al_2O_3 (or Ni/γ-Al_2O_3) bed was 30 mm, while the length of the discharge was 150 mm in these three packing modes.

Gas analysis and parameter definition

The gas products were analyzed by a two-channel gas chromatography (GC, Shimadzu GC2014) equipped with a thermal conductivity detector (TCD) and a flame ionization detector (FID) and. Each measurement was repeated three times when the reaction reached to a steady state. In this work, ozone

and carbon deposition were not detected. The conversion of CO_2 (C), CO selectivity (S) and the energy efficiency of the plasma process (η) were determined by Equations 9 to 11, respectively:

$$C_{CO_2}(\%) = \frac{CO_2 \text{ converted } (mol/s)}{CO_2 \text{ introduced } (mol/s)} \times 100 \quad (9)$$

$$S_{CO}(\%) = \frac{CO \text{ produced } (mol/s)}{CO_2 \text{ converted } (mol/s)} \times 100 \quad (10)$$

$$\eta(\%) = \frac{CO_2 \text{ flow rate } (ml/s) \cdot C_{CO_2}(\%) \cdot \Delta H (kJ/mol)}{22.4 \times \text{Discharge power } (W)} \quad (11)$$

The CO selectivity is close to 1, which suggests the CO is the major carbon containing product in the plasma conversion.

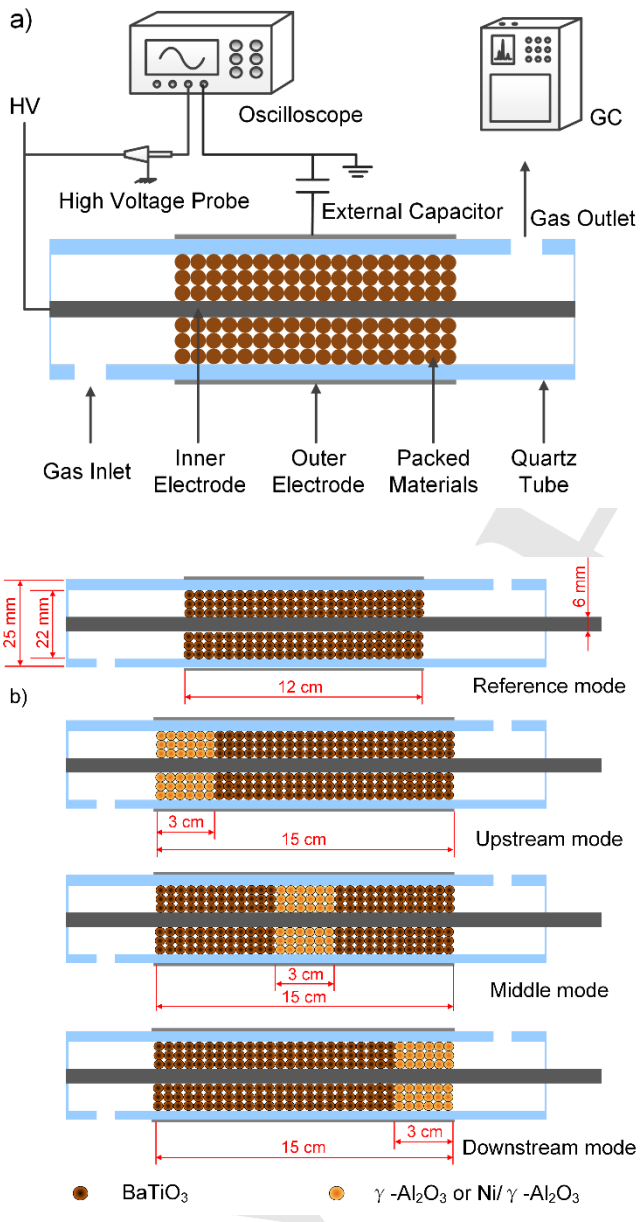

Figure 5. Schematic diagram of a) the experimental setup and b) different packing modes.

Acknowledgements

The financial support of this work by the EPSRC SUPERGEN Hydrogen & Fuel Cell (H2FC) Programme (Ref. EACPR_PS5768) and the EPSRC CO2Chem Seedcorn grant is gratefully acknowledged.

Keywords: plasma-catalysis • non-thermal plasma • dielectric barrier discharge • packed-bed • CO_2 conversion

[1] The State of Greenhouse Gases in the Atmosphere Based on Global Observations through 2013, *World Meteorological Organization*, **2014**, pp.1-10.

[2] EurObserv' ER Biogas barometer, **2012**.

[3] aE. V. Kondratenko, G. Mul, J. Baltrusaitis, G. O. Larrazabal, J. Perez-Ramirez, *Energy Environ. Sci.* **2013**, *6*, 3112-3135; bM. Mikkelsen, M. Jorgensen, F. C. Krebs, *Energy Environ. Sci.* **2010**, *3*, 43-81.

[4] J. Medina-Ramos, R. C. Pupillo, T. P. Keane, J. L. DiMeglio, J. Rosenthal, *J. Am. Chem. Soc.* **2015**, *137*, 5021-5027.

[5] aS. Paulussen, B. Verheyde, X. Tu, C. De Bie, T. Martens, D. Petrovic, A. Bogaerts, B. Sels, *Plasma Sources Sci. Technol.* **2010**, *19*, 034015; bS. Mahammadunnisa, E. L. Reddy, D. Ray, C. Subrahmanyam, J. C. Whitehead, *Int. J. Greenhouse Gas Control* **2013**, *16*, 361-363.

[6] aX. Tu, J. C. Whitehead, *Appl Catal B-Environ* **2012**, *125*, 439-448; bW. Wang, B. Patil, S. Heijkers, V. Hessel, A. Bogaerts, *ChemSusChem* **2017**, *10*, 2145-2157.

[7] aR. Aerts, R. Snoeckx, A. Bogaerts, *Plasma Process. Polym.* **2014**, *11*, 985-992; bF. Brehmer, S. Welzel, M. C. M. van de Sanden, R. Engeln, *J. Appl. Phys.* **2014**, *116,* 123303; cR. Aerts, W. Somers, A. Bogaerts, *ChemSusChem* **2015**, *8*, 702-716; dX. Duan, Y. Li, W. Ge, B. Wang, *Greenh. Gases* **2015**, *5*, 131-140; eM. Ramakers, I. Michielsen, R. Aerts, V. Meynen, A. Bogaerts, *Plasma Process. Polym.* **2015**, *12*, 755-763; fI. Belov, S. Paulussen, A. Bogaerts, *Plasma Sources Sci. Technol.* **2016**, *25*, 015023; gI. Belov, J. Vanneste, M. Aghaee, S. Paulussen, A. Bogaerts, *Plasma Process. Polym.* **2016**; hD. Mei, Y.-L. He, S. Liu, J. Yan, X. Tu, *Plasma Process. Polym.* **2016**, *13*, 544-556; iA. Ozkan, T. Dufour, A. Bogaerts, F. Reniers, *Plasma Sources Sci.Technol.* **2016**, *25*, 045016; jA. Ozkan, T. Dufour, T. Silva, N. Britun, R. Snyders, A. Bogaerts, F. Reniers, *Plasma Sources Sci. Technol.* **2016**, *25*, 025013; kR. X. Li, Q. Tang, S. Yin, T. Sato, *Appl. Phys. Lett.* **2007**, *90,* 131502; lS. Wang, Y. Zhang, X. Liu, X. Wang, *Plasma Chem. Plasma Process.* **2012**, *32*, 979-989; mQ. Q. Yu, M. Kong, T. Liu, J. H. Fei, X. M. Zheng, *Plasma Chem. Plasma Process.* **2012**, *32*, 153-163; nM. A. Lindon, E. E. Scime, *Frontiers in Physics* **2014**, *2*, article 55; oX. F. Duan, Z. Y. Hu, Y. P. Li, B. W. Wang, *AiCHE J* **2015**, *61*, 898-903; pD. H. Mei, X. B. Zhu, Y. L. He, J. D. Yan, X. Tu, *Plasma Sources Sci. Technol.* **2015**, *24*, 015011; qK. Van Laer, A. Bogaerts, *Energy Technol.* **2015**, 1038-1044; rT. Butterworth, R. Elder, R. Allen, *Chem. Eng. J.* **2016**, *293*, 55-67; sX. Zhu, X. Tu, D. Mei, C. Zheng, J. Zhou, X. Gao, Z. Luo, M. Ni, K. Cen, *Chemosphere* **2016**, *155*, 9-17; tD. Ray, C. Subrahmanyam, *RSC Adv.* **2016**, *6*, 39492-39499.

[8] aW. Xu, M. W. Li, G. H. Xu, Y. L. Tian, *Jpn J. Appl. Phys.* **2004**, *43*, 8310-8311; bG. Horvath, J. D. Skalny, N. J. Mason, *J. Phys. D Appl. Phys.* **2008**, *41,* 225207.

[9] aP. G. Reyes, E. F. Mendez, D. Osorio-Gonzalez, F. Castillo, H. Martinez, *Phys. Status. Solidi. C* **2008**, *5*, 907-910; bS. L. Brock, T. Shimojo, M. Marquez, C. Marun, S. L. Suib, H. Matsumoto, Y. Hayashi, *J. Catal.* **1999**, *184*, 123-133.

[10] aA. Indarto, D. R. Yang, J. W. Choi, H. Lee, H. K. Song, *J. Hazard. Mater.* **2007**, *146*, 309-315; bS. C. Kim, M. S. Lim, Y. N. Chun, *Plasma Chem. Plasma Process.* **2014**, *34*, 125-143; cT. G. Nunnally, K.; Rabinovich, A.; Fridman, A.; Gutsol, A.; Kemoun, A., *J. Phys. D Appl. Phys.* **2011**, *44*, 274009; dM. Ramakers, G. Trenchev, S. Heijkers, W. Wang, A. Bogaerts, *ChemSusChem* **2017**, *10*, 2642-2652.

[11] aH. S. Uhm, H. S. Kwak, Y. C. Hong, *Environ. Pollut.* **2016**, *211*, 191-197; bG. Chen, V. Georgieva, T. Godfroid, R. Snyders, M.-P. Delplancke-Ogletree, *Appl. Catal. B: Environ.* **2016**, *190*, 115-124.

[12] K. Zhang, G. Zhang, X. Liu, A. N. Phan, K. Luo, *Ind. Eng. Chem. Res.* **2017**, *56*, 3204-3216.
[13] aS. G. Wang, D. B. Cao, Y. W. Li, J. Wang, H. Jiao, *J. Phys. Chem. B* **2005**, *109*, 18956-18963; bC. Liu, T. R. Cundari, A. K. Wilson, *The J. Phys. Chem. C* **2012**, *116*, 5681-5688.
[14] aY. Zeng, X. Tu, *J. Phys. D: Appl. Phys.* **2017**, *50*, 184004; bD. Mei, B. Ashford, Y.-L. He, X. Tu, *Plasma Process. Polym.* **2017**, *14*, e1600076.
[15] aM. K. Nikoo, N. A. S. Amin, *Fuel Process. Technol.* **2011**, *92*, 678-691; bW. Wang, M. Rong, Y. Wu, J. D. Yan, *J.Phys. D: Appl. Phys.* **2014**, *47*, 255201; cW. Wang, A. Bogaerts, *Plasma Sources Sci.Technol.* **2016**, *25*, 055025.
[16] W. Wang, D. Mei, X. Tu, A. Bogaerts, *Chem. Eng. J.* **2017**, *330*, 11-25.
[17] D. Mei, X. Tu, *J.CO2 Util.* **2017**, *19*, 68-78.
[18] Y. Z. Wen, X. Z. Jiang, *Plasma Chem.Plasma Process.* **2001**, *21*, 665-678.
[19] D. Mei, X. Zhu, C. Wu, B. Ashford, P. T. Williams, X. Tu, *Appl. Catal.B: Environ.* **2016**, *182*, 525-532.
[20] E. Jwa, S. B. Lee, H. W. Lee, Y. S. Mok, *Fuel Process. Technol.* **2013**, *108*, 89-93.
[21] aC. J. Liu, J. J. Zou, K. L. Yu, D. G. Cheng, Y. Han, J. Zhan, C. Ratanatawanate, B. W. L. Jang, *Pure Appl. Chem.* **2006**, *78*, 1227-1238; bC. J. Liu, M. Y. Li, J. Q. Wang, X. T. Zhou, Q. T. Guo, J. M. Yan, Y. Z. Li, *Chin. J. Catal.* **2016**, *37*, 340-348.
[22] aT. Nozaki, K. Okazaki, *Green Process. Syn.* **2012**, *1*, 517-523; bH. L. Chen, H. M. Lee, S. H. Chen, M. B. Chang, *Ind. Eng. Chem. Res.* **2008**, *47*, 2122-2130; cA. Mizuno, *Catal. Today* **2013**, *211*, 2-8.
[23] R. Aerts, T. Martens, A. Bogaerts, *J. Phys. Chem. C* **2012**, *116*, 23257-23273.
[24] R. Snoeckx, Y. X. Zeng, X. Tu, A. Bogaerts, *RSC Adv.* **2015**, *5*, 29799-29808.
[25] X. Tu, H. J. Gallon, J. C. Whitehead, *Catal. Today* **2013**, *211*, 120-125.

ARTICLE

The location of the catalyst bed in the packed-bed DBD reactor plays a crucial role in determining the performance of the plasma CO_2 conversion. Argon plasma treatment of the reacted Ni catalyst showed higher CO_2 conversion compared to untreated catalyst.

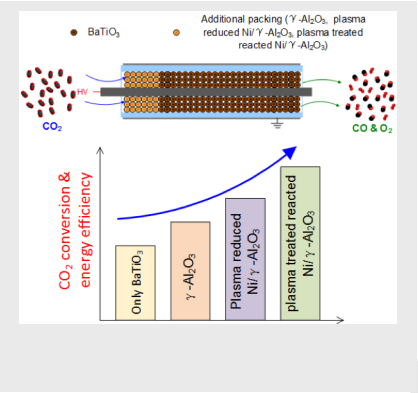

*Danhua Mei, and Xin Tu**

Page No. – Page No.

Atmospheric pressure non-thermal plasma activation of CO_2 in a packed-bed dielectric barrier discharge reactor